ELSEVIER

Applied Mathematical Modelling 24 (2000) 27–43

APPLIED MATHEMATICAL MODELLING

www.elsevier.nl/locate/apm

An optimal trace zinc biomonitor (*Haliotis diversicolor supertexta*) control system design in aquacultural ecosystems

Chung-Min Liao *, Bo-Ching Chen, Ming-Chao Lin, Jein-Wen Chen

Department of Agricultural Engineering, National Taiwan University, Taipei, 10617 Taiwan, ROC

Received 13 July 1998; received in revised form 12 May 1999; accepted 7 June 1999

Abstract

The purpose of this paper is to synthesize an optimal trace metal biomonitor control system to efficiently manage aquacultural water quality. A biomonitor organism of gastropod mollusc *Haliotis diversicolor supertexta* was chosen to estimate zinc (Zn) bioaccumulation. The bioaccumulation dynamics of Zn by *H. diversicolor supertexta* from an alga *Gracilaria tenuistipitata* var. *liui* and ambient water in aquaculture ponds is developed based on a six-compartment pharmacokinetic model. A linear control model based on the dynamic bioaccumulation model is developed to design an optimal feedback biomonitor control system. Linear quadratic regulators (LQRs) with output feedback control of a linear-invariant system are assigned for design algorithm and an optimal proportional plus integral (PI) feedback control strategy is synthesized. Numerical results from the model implementation show that the optimal selection of tuning parameters and the resulting costs vary with desired equilibrium state. The designed optimal feedback biomonitor control system, when suitably tuned, gives a satisfactory monitor of mollusc Zn bioaccumulation. The biomonitor control system developed accounting for bioaccumulation dynamics of Zn in the target tissues of molluscs can be used in the future to evaluate the effects of suspended solid removal devices and biofilters and/or other control scenarios on water quality management in aquacultural ecosystems. © 2000 Elsevier Science Inc. All rights reserved.

Keywords: Aquaculture; Bioaccumulation; Biomonitor; Mollusc; Optimal feedback control

1. Introduction

Bioaccumulation is the result of uptake chemical by aquatic organisms from and elimination to the ambient water environment. Bioaccumulation may result in concentrations of toxic chemicals in fish/shellfish that are large multiples of those of the water in which the fish/shellfish dwell. Therefore, bioaccumulation plays an important role in hazardous assessment procedures in water quality management. The ability to predict this bioaccumulation is thus important for improving the risk assessment to biota and humans caused by contaminants in aquatic systems.

For the contaminant management in aquaculture ponds, it is important to be able to predict the impact of chemical and toxic effects in aquacultural species. Building such a

* Corresponding author. Fax: +886-2-23626433.
E-mail address: hml@watgis.ae.ntu.edu.tw (C.-M. Liao).

PII: S0307-904X(99)00024-4

predictive capability requires knowledge of the transport of the chemical from its origin into the species and of the interaction of the chemical with crucial target tissues in the species.

The uptake and subsequent internal transport models of chemicals from water and food by fish have been the subject of a number of studies and are well documented [1]. To date, however, these types of models have not often been applied to the estimation of chemical bioaccumulation and detoxification in the molluscs such as gastropods and bivalve.

Gastropods and bivalve are excellent bioaccumulators of a wide range of pollutants and the levels of accumulation in their tissues are considered to reflect the bioavailable components of chemicals in aquatic systems [2–4]. They are either filter feeders, herbivores or carnivores and have the potential to bioaccumulate contaminants that would normally be present in water or within sediments. They are also ideal species for environmental monitoring, because their sedentary nature does not require consideration of complex migratory factors in the interpretation of the bioaccumulation data [3,5].

It is generally recognized that gastropods and bivalve represent the most important source of heavy metals to human populations [6–8]. The potential hazards associated with heavy metal poisoning, however, are not restricted to polluted lakes and rivers. Elevated heavy metal concentrations in shellfish have often been reported in lakes far from direct sources of heavy metal pollution. The health risk associated with heavy metal intoxication to humans together with the global heavy metal contamination of aquatic ecosystems necessitates the development of models to predict heavy metal dynamics in molluscs.

The effective use of a biomonitor depends on the development of models that permit us to relate metal concentrations in the aquatic environment to those in the organism chosen as a biomonitor, i.e., a simple relationship should exist between its trace metal content and the concentration of the metal in its environment. A good biomonitor should also be easy to collect, widespread and abundant, tolerant of a wide range of chemical conditions, and to provide sufficient tissue for contaminant analysis. Croteau et al. [9] and Martin and Coughtrey [10] suggested that molluscs could be used as metal biomonitors.

Curtis [11] and Livingstone [12] reported that mantle soft tissue of gastropod molluscs is the site of shell deposition and contains mixed-function oxidases for the detoxification of aliphatic hydrocarbons and other toxic contaminants. Walsh et al. [13] further indicated that mollusc might utilize the deposition process of new shell material to relocate bioaccumulated contaminants from the metabolically active soft tissue to the relatively inert shell material. The present study has taken into account the metal transport through soft tissue wall and blood to the shell. The shell acts as a storage matrix for trace metals.

The bioaccumulation of metal zinc (Zn) in the gastropod mollusc *Haliotis diversicolor supertexta* and the red alga *Gracilaria tenuistipitata* var. *liui* was to be dynamically modeled and an optimal biomonitor control system was to be synthesized in an aquacultural ecosystem. Zn is of particular ecotoxicological concern where Zn accumulation and toxicity is of considerable interest due to the carcinogenic risks associated with Zn exposure [14]. The alga *G. tenuistipitata* var. *liui* is the major forage for culturing the mollusc *H. diversicolor supertexta*. These two aquacultural species are considered to be the important economic aquatic products in Taiwan region. *H. diversicolor supertexta* is appreciated for its delicacy and high market value, the aquaculture of *H. diversicolor supertexta* is a promising business in Taiwan.

This aim of this paper is to investigate the water quality management of mollusc metal bioaccumulation in aquaculture systems from the viewpoint of linear control theory and to show how ideas from engineering sciences might be used to design an optimal biomonitor control system for fishery management strategies.

2. Model structure

2.1. Model assumption

Before deriving system equations to describe the dynamic behavior of trace Zn bioaccumulation in mollusc target tissues, the following assumptions are made to simplify the certain physical and biological aspects.

(1) *Finite compartmental model*. There is a six-compartment pharmacokinetic model of blood–gill–soft tissue–gut wall–alimentary canal–shell, representing actual anatomical units of *H. diversicolor supertexta*.

(2) *A gill transport system*. There is a gill transport system. It is assumed that the gill acts as a continuous-stirred tank reactor or well-mixed compartment into and out of which water flows, with chemical and oxygen being transferred to the mollusc based on diffusive mass transfer. A ventilation flow rate Q_w gives the input respired water flow rate. The total water flow is steady and uniformly distributed among the water channels.

(3) *Blood flow transport system*. There is a blood transport system. A flow rate $Q_{ij} \geqslant 0$ gives the blood flow from the jth blood compartment to the ith organ compartment for $i \neq j$ with $1 \leqslant i, j \leqslant n$. All transport occurs by blood flows, i.e., intercompartment transport by direct diffusion is negligible. The blood flow is steady and uniformly distributed among the blood channels.

(4) *Chemical equilibrium*. There is a complete equilibrium of chemical between the blood phase and the tissue phase of each compartment. It is assumed that there is an inert soluble chemical with blood-chemical partitioning/binding coefficient f_i present in the amount of chemical partitioned to compartment tissue i. Therefore, the transport is flow limited in the sense that chemical in the blood leaving a region is in equilibrium with the region.

(5) *Mass balance of chemical substance*. There is a local mass balance of chemical substance in that for each compartment the amount of chemical substance entering is equal to the amount leaving. Chemical with the compartment is assumed to be at steady state. This can be interpreted as the changes in the amount of chemical partitioned to each compartment tissue are assumed to take place relatively quickly upon a change in input variables.

(6) *Mass balance of blood flow*. There is a local mass balance of blood flow in that

$$\sum_{\substack{j=0 \\ j\neq i}}^{n} Q_{ij} = \sum_{\substack{j=0 \\ j\neq i}}^{n} Q_{ji} \quad \text{for } 1 \leqslant i \leqslant n.$$

2.2. System model

The mollusc *H. diversicolor supertexta* absorbs Zn directly from the water via the gills and through the consumption of food, the red alga *G. tenuistipitata* var. *liui*, into the alimentary canal with exchange to the gut tissue and subsequent exchange with the blood. The blood exchanges with the gill, shell, gut wall, and soft tissue compartments. Zn loss can occur via the gills to the water, via egestion of fecal matter, growth dilution or as a result of metabolic transformation. Fig. 1 shows the conceptual diagram of pathways of Zn intake and elimination considered for an aquacultural *H. diversicolor supertexta*. A conceptual physiologically based pharmacokinetic (PBPK) model of bioaccumulation of Zn in a mollusc key tissue is illustrated in Fig. 2 in that the size of the tissue compartment represents storage capacity dependent on anatomical volume and metal partitioning, and the size of the conduits represent flows dependents on the listed parameters.

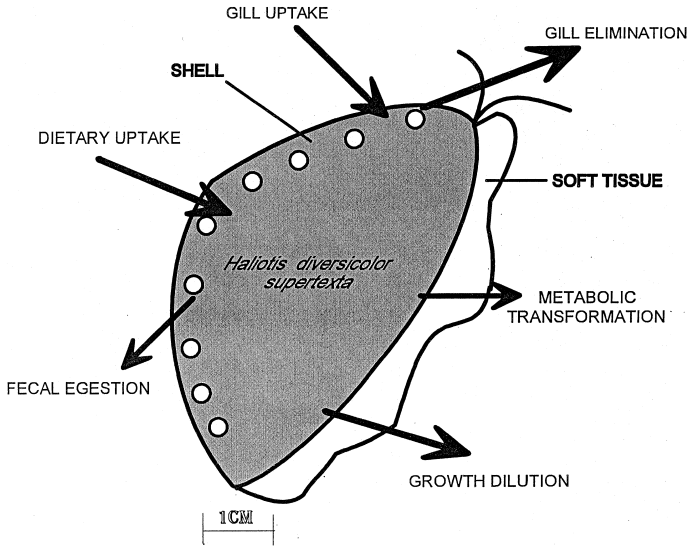

Fig. 1. Schematic diagram of pathways of Zn intake and elimination considered for an aquacultural mollusc, *Haliotis diversicolor supertexta*.

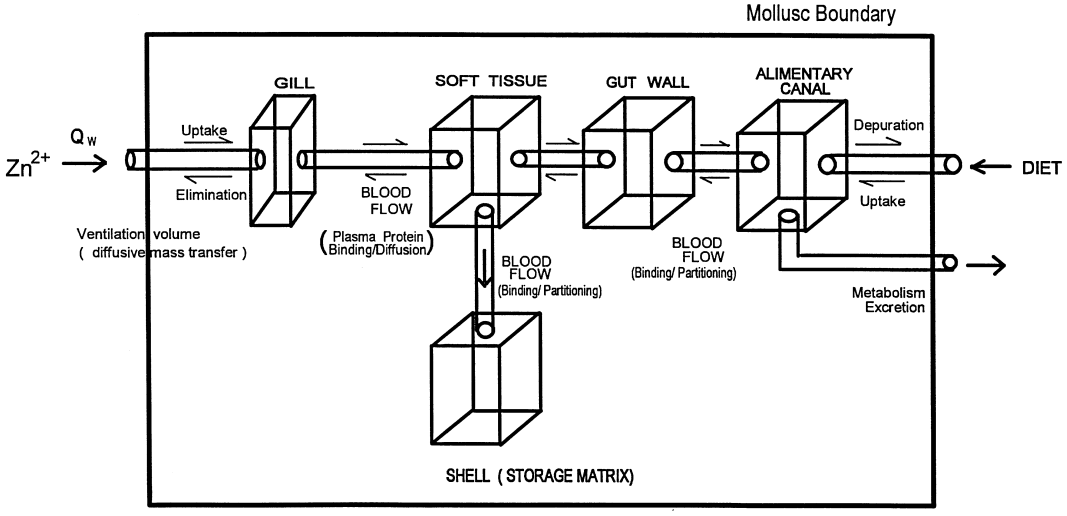

Fig. 2. Schematic diagram of physiologically based pharmacokinetic model of Zn bioaccumulation in a mollusc key compartments.

Based on model assumption (1), *H. diversicolor supertexta* could be pharmacokinetically modeled as a six-compartment of blood – gill – soft tissue – alimentary canal – gut wall – shell as well as one algae compartment to represent the principal features of the bioaccumulation and transport of Zn in the mollusc (Fig. 3). Applying of a mass balance relation to each organ compartment in Fig. 3 yields the following dynamic equations:

$$V_1 \frac{dC_1}{dt} = Q_{21}(C_{d2} - f_d C_1) + Q_{31}(C_{d3} - f_d C_1) + Q_{41}(C_{d4} - f_d C_1) + Q_{61}(C_{d6} - f_d C_1),$$

$$W_2 \frac{dC_2}{dt} = Q_{2w}(\alpha_{w2} C_w - C_{d2}) + Q_{21}(f_d C_1 - C_{d2}),$$

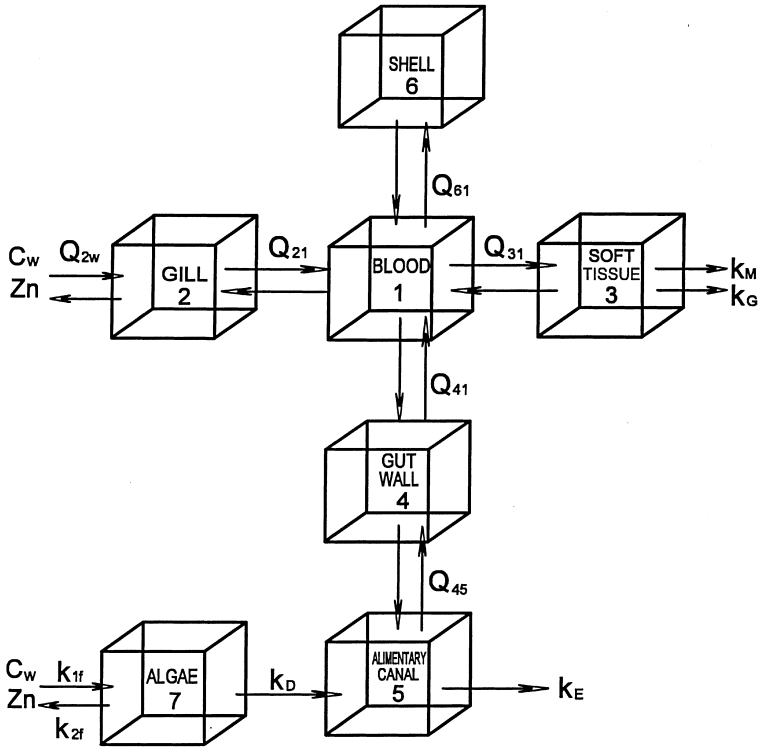

Fig. 3. Schematic diagram of six-compartment pharmacokinetic model of Zn for the biomonitor (*Haliotis diversicolor supertexta*) and for one-compartment of the alga (*Gracilaria tenuistipitata* var. *liui*).

$$
\begin{aligned}
W_3\frac{dC_3}{dt} &= Q_{31}(f_dC_1 - C_{d3}) - K_MW_3C_3 - K_GW_3C_3,\\
W_4\frac{dC_4}{dt} &= Q_{41}(f_dC_1 - C_{d4}) + Q_{45}(C_{d5} - \beta_{45}C_{d4}),\\
W_5\frac{dC_5}{dt} &= K_DW_tC_7 + Q_{45}(\beta_{45}C_{d4} - C_{d5}) - K_EW_tC_5,\\
W_6\frac{dC_6}{dt} &= Q_{61}(f_dC_1 - C_{d6}),\\
W_7\frac{dC_7}{dt} &= k_{1f}W_7C_w - k_{2f}W_7C_7 - K_DW_tC_7,
\end{aligned}
\tag{1}
$$

where Q_{ij} is the diffusive exchange rate between compartments i and j (l d^{-1}), C_{di} the dissolved Zn concentration in compartment i (g l^{-1}), C_1 the total Zn concentration in the blood (g g^{-1}), C_w the Zn concentration in the water (g l^{-1}), V_1 the blood volume (l), f_d the binding coefficient of Zn concentration to plasma proteins (g l^{-1}), W_i the time-independent tissue weight of compartment i (g[dry]), W_t the whole mollusc weight (g[dry]), C_i the Zn concentration of the compartment i (g g^{-1}), α_{w2} the gill sorption factor representing enhancement of surface sorption, β_{45} the bile factor representing enhancement of exchange gut to alimentary canal, K_E the elimination rate of fecal egestion (g g^{-1} d^{-1}), K_M the metabolic transformation rate of Zn (g g^{-1} d^{-1}), K_D the Zn uptake rate from algae (g g^{-1}d^{-1}), K_G the mollusc growth dilution rate (g g^{-1}d^{-1}), k_{1f} the Zn uptake rate of algae (l g^{-1} d^{-1}), and k_{2f} is the Zn elimination rate of algae (g g^{-1} d^{-1}).

Applying model assumption (4) of chemical equilibrium to the relations between the dissolved Zn concentration in a specific compartment and the concentration of total Zn in that compartment gives the following expression,

$$f_i = \frac{C_i}{C_{\mathrm{di}}}, \tag{2}$$

where f_i is the partition coefficient or is referred to as a tissue/blood equilibrium distribution ratio for linear binding (l g^{-1}). This expression is then substituted into each of the diffusive exchange terms.

After some mathematical manipulations, Eq. (1) incorporating with Eq. (2) yields a state-space realization form of a linear dynamic equation,

$$\left\{\frac{\mathrm{d}C(t)}{\mathrm{d}t}\right\} = [K]\{C(t)\} + [B]\{q(t)\}, \tag{3}$$

where $\{C(t) = C_1(t)\ C_2(t)\ C_3(t)\ C_4(t)\ C_5(t)\ C_6(t)\ C_7(t)\}^{\mathrm{T}}$ (g g^{-1}) represents a state variable vector of Zn concentrations in blood, gill, soft tissue, gut wall, alimentary canal, shell and algae compartments, respectively; $\{q(t)\} = \{C_{\mathrm{w}}(t)\ 0\ 0\ 0\ 0\ 0\ 0\}^{\mathrm{T}}$ (g l^{-1}) represents an input vector of Zn concentrations in ambient water, while state matrix $[K]$ (d^{-1}) and constant input matrix $[B]$ (l g^{-1} d^{-1}) have the following forms, respectively as,

$$[K] = \begin{bmatrix} k_{11} & \cdots & k_{17} \\ \vdots & \ddots & \vdots \\ k_{71} & \cdots & k_{77} \end{bmatrix}$$

$$= \begin{bmatrix}
-(Q_{21}+Q_{31}+Q_{41}+Q_{61})\frac{f_d}{V_1} & \frac{Q_{21}}{f_2V_1} & \frac{Q_{31}}{f_3V_1} & \frac{Q_{41}}{f_4V_1} & 0 & \frac{Q_{61}}{f_6V_1} & 0 \\
\frac{Q_{21}f_d}{W_2} & -\left(\frac{Q_{2w}}{f_2W_2}+\frac{Q_{21}}{f_2W_2}\right) & 0 & 0 & 0 & 0 & 0 \\
\frac{Q_{31}f_d}{W_3} & 0 & -\left(\frac{Q_{31}}{f_3W_3}+K_{\mathrm{G}}+K_{\mathrm{M}}\right) & 0 & 0 & 0 & 0 \\
\frac{Q_{41}f_d}{W_4} & 0 & 0 & -\left(\frac{Q_{41}}{f_4W_4}+\frac{Q_{45}\beta_{45}}{f_4W_4}\right) & \frac{Q_{45}}{f_5W_4} & 0 & 0 \\
0 & 0 & 0 & \frac{Q_{45}\beta_{45}}{f_4W_5} & -\left(\frac{Q_{45}}{f_5W_5}+\frac{K_{\mathrm{E}}W_t}{W_5}\right) & 0 & K_{\mathrm{D}}\frac{W_t}{W_5} \\
\frac{Q_{61}f_d}{W_6} & 0 & 0 & 0 & 0 & -\frac{Q_{61}}{f_6W_6} & 0 \\
0 & 0 & 0 & 0 & 0 & 0 & -\left(k_{2f}+\frac{W_t}{W_7}K_{\mathrm{D}}\right)
\end{bmatrix} \tag{4}$$

and

$$[B] = \begin{bmatrix} \frac{Q_{2w}\alpha_{w2}}{W_2} \\ 0 \\ 0 \\ 0 \\ 0 \\ 0 \\ k_{1f} \end{bmatrix}. \tag{5}$$

For the two compartments of gill and alimentary canal that interact with Zn in external water and food, additional processes have to be considered. For the gill, an increased surface sorption to the gill surface was necessary. The exchange of Zn between internal gill tissue and the blood was therefore set at a lower exchange than the exchange between the gill surface and the water. For the Zn in the alimentary canal contents and its exchange with the gut wall, the input from Zn in the algae and Zn egested in feces were included together with an enhanced exchange between the gut and alimentary canal to present direct biliary transfer of Zn from the gut to gut contents.

3. Optimal biomonitor control system synthesis

3.1. System control model

A derivative variable can be defined as, $\Delta y_i = y_i - y_{is}$, in which y_i is the ith element of vector $\{y\}$, and Δy_i is the difference between y_i and a steady-state value or a set point, y_{is}. By introducing the derivative variables into Eq. (3), a mollusc Zn bioaccumulation model based on a six-compartment PBPK model (Fig. 3) can then be obtained as,

$$\left\{\frac{\mathrm{d}X(t)}{\mathrm{d}t}\right\} = [K]\{X(t)\} + [B]\{U(t)\} \tag{6}$$

in which $\{X\} = \{\Delta C\} = \{C\} - \{C_s\}$, a system state variable vector, and $\{U\} = \{\Delta q\} = \{q\} - \{q_s\}$, a system controllable input vector.

Practically it is not always possible to have all the state variables available for feedback. Rather than reconstructing the state variables via a Kalman filter or some form of a state estimator, it is preferable to generate the control variables by taking linear combinations of the available output variables. The state output vector of interest to the problem is, $\{Z(t)\} = [H]\ \{X(t)\}$, where $\{Z(t)\}$ is the state output (measurement) variable vector, and $[H]$ is a constant matrix of output (measurement) state vector.

Therefore, when considering the linear dynamic bioaccumulation model in Eq. (6), a system control model is obtained as follows:

$$\begin{aligned} &\left\{\dot{X}(t)\right\} = [K]\{X(t)\} + [B]\{U(t)\}, \\ &\{Z(t)\} = [H]\{X(t)\}. \end{aligned} \tag{7}$$

Eq. (7) can be employed in the bioaccumulation dynamic analysis and control of trace metals in molluscs from water and food in an aquacultural ecosystem. The concept of stability is extremely important since every workable system must be designed to be stable. The elements of $\{X(t)\}$ will remain bounded only if $R_e(\lambda_k) \leqslant 0$ for all k, where λ_k are the eigenvalues of matrix $[K]$ [15–17].

3.2. Optimal feedback control strategy

A more general form of the system control model in Eq. (7) may be expressed as:

$$\begin{aligned} &\left\{\dot{X}(t)\right\} = [K]\{X(t)\} + [B]\{U(t)\}, \\ &\{X(0)\} = \{X_0\}, \quad \{U(0)\} = \{U_0\}, \\ &\{Z(t)\} = [H]\{X(t)\}. \end{aligned} \tag{8}$$

The performance index of control can then be measured by a quadratic cost function based on the integral of the squared error in a linear quadratic regulator (LQR) scheme as,

$$\begin{aligned} J &= \frac{1}{2}\int_0^{t_f} \left(\{Z(t)\}^{\mathrm{T}}[S]\{Z(t)\} + \{\dot{U}(t)\}^{\mathrm{T}}[R]\{\dot{U}(t)\}\right)\mathrm{d}t \\ &= \frac{1}{2}\int_0^{t_f} \left(\{X(t)\}^{\mathrm{T}}[Q]\{X(t)\} + \{\dot{U}(t)\}^{\mathrm{T}}[R]\{\dot{U}(t)\}\right)\mathrm{d}t, \end{aligned} \tag{9}$$

where $[Q] = [H]^{\mathrm{T}}[S][H]$, in which $[S]$ is a positive semidefinite weighting matrix, and $[R]$ is a positive definite control weighting matrix.

To ensure that the controller can drive the system for a specific period of time, the system must be controllable. To control the system, the performance with feedback must be monitored, thus the system must be observable. If the linear control model in Eq. (7) is observable, then $[Q]=[H]^{\mathrm{T}}[S][H]$ is a positive semidefinite weighting matrix when $[S]$ is positive semipositive. Observability and controllability of the control model are guaranteed if and only if the following matrices,

$$\begin{aligned}[\Xi(t)] &= \left[[H]^{\mathrm{T}}|[K]^{\mathrm{T}}[H]^{\mathrm{T}}|\cdots|\left([K]^{(n-1)}\right)^{\mathrm{T}}[H]^{\mathrm{T}}\right],\\ [\Theta(t)] &= \left[[B]|[K][B]|\cdots|[K]^{(n-1)}[B]\right]\end{aligned} \tag{10}$$

have rank n (i.e., $|[\Xi][\Xi]^{\mathrm{T}}|\neq 0$, and $|[\Theta][\Theta]^{\mathrm{T}}|\neq 0$), respectively.

The solution of the optimal controllable vector ($\{\hat{U}(t)\}$) which minimized cost function in Eq. (9) can be given by the following expression as (see Appendix A),

$$\{\hat{U}(t)\} = [[L_{12}]+[L_{22}]][H]\{\hat{X}(t)\} + [[L_{11}]+[L_{21}]][H]\int_0^t \{\hat{X}(\tau)\}\,\mathrm{d}\tau. \tag{11}$$

Eq. (11) is a basic linear feedback control law throughout the model. The elements $[L_{ij}]$ in Eq. (11) are appropriately partitioned submatrices of $\left[-[R]^{-1}[B_a]^{\mathrm{T}}[P^*][H_a]^{-1}\right]$ where $[B_a]=[[0]|[B]]^{\mathrm{T}}$, $[H_a]=\mathrm{diag}[[H]|[H]]$, and $[P^*]=[P^*]^{\mathrm{T}}$ is the unique, positive definite solution of the following algebraic Riccati equation: $-[P^*][K_a]-[K_a]^{\mathrm{T}}[P^*]+[P^*][B_a][R]^{-1}[B_a]^{\mathrm{T}}[P^*]-[Q_a]=0$ in which

$$[K_a]=\begin{bmatrix}[0] & [I]\\ [0] & [K]\end{bmatrix}$$

and $[Q_a]=\mathrm{diag}[[Q]|[0]]$. This is the desired optimal feedback controller to the original LQR as defined in Eqs. (8) and (9): a modern control theory method for designing the proportional plus integral (PI) feedback controller. Fig. 4 shows the structure of an optimal PI feedback control strategy for the trace metal biomonitor system considered.

4. Model implementation

4.1. Input parameters

The model is composed of terms involving mollusc weight and bioenergetics and terms involving physiological metal-specific processes. Input parameters for the model implementation were determined in the following way.

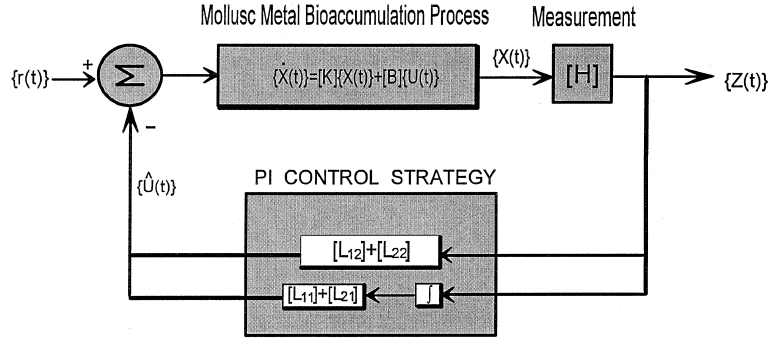

Fig. 4. Structure of an optimal PI feedback control strategy for the trace metal biomonitor control system.

For the bioenergetic behavior, data were generally available for the fish to estimate the parameters. Because no general equations for the molluscs could be found, it is assumed that equations used to estimate bioenergetics for fish were also suitable for that of molluscs. Table 1 lists the formula used to calculate bioenergetic parameters for rate constants of dietary uptake, elimination, growth dilution, and metabolic transformation for *H. diversicolor supertexta*.

The data for weights of *H. diversicolor supertexta* were adopted from the laboratory measurements done by Lin and Liao [18]. Table 2 gives the resulting mollusc weights and bioenergetic parameters used in the model implementation.

It is not possible to estimate all of the physiological parameters for the model independently of the experimental data because individual experiments for *H. diversicolor supertexta* were not available. It is possible, however, to estimate from the literature, the order of parameters for the various organs and the fraction of Zn in the blood in the available plasma form. Therefore, a preliminary database adapted from Thomann et al. [19] regarding the trace cadmium

Table 1
Equations used to compute bioenergetic parameters of rate constants of k_D, k_E, k_M, and k_G

Transfer mechanism	Formula
Metabolic transformation[a]	$k_M = 0.693 t_{1/2}^{-1}$
Dietary uptake[b]	$k_D = E_D F_D W_M^{-1}$, $E_D^{-1} = 5.3(\pm 1.5) \times 10^{-8} K_{ow} + 2.3(\pm 0.3)$, $F_D = 0.022 W_M^{0.85} \exp(0.06T)$
Elimination by fecal egestion[c]	$k_E = 0.25 k_D$
Growth dilution[d]	$k_G = 0.00251 W_M^{-0.2}$, $T \approx 25°C$, $k_G = 0.000502 W_M^{-0.2}$, $T \approx 10°C$

[a] $t_{1/2}$ = half-life of chemical.
[b] E_D is the dietary uptake efficiency, F_D the food ingestion rate (kg food d^{-1}), W_M the mollusc weight (kg[dry]), K_{ow} the chemical octanol–water partition coefficient, and T is the water temperature (°C) [24,25].
[c] Adapted from Gobas et al. [24].
[d] Adapted from Thomann and Connolly [26].

Table 2
Properties of molluscan shellfish used in model implementation and resulting values for k_{1f}, k_{2f}, k_D, k_E, k_M, and k_G

Whole mollusc weight (not including shell) $W_t = 2.5$ g[dry][a]	
Blood volume $V_1 = 0.02$ ml[b]	
Weight of gill $W_2 = 0.0196$ g[dry][a]	
Weight of soft tissue $W_3 = 2.3608$ g[dry][a]	
Weight of gut wall $W_4 = 0.01$ g[dry][a]	
Weight of alimentary canal contents $W_5 = 0.02$ g[dry][a]	
Weight of shell $W_6 = 2.5136$ g[dry][a]	
Weight of red algae $W_7 = 1.08$ g[dry][a]	
Chemical octanol–water partition coefficient $K_{ow} < 10^6$	
Water temperature $T = 25°C$	
Chemical half-life $t_{1/2} > 5$ yrs	
Zn in pond water $C_w = 1$ mg l^{-1}[a]	
Resulting values	
$k_{1f} = 0.0123$ l g^{-1} d^{-1} [a]	
$k_{2f} = 0.58$ d^{-1} [a]	
$k_M \ll 0.00038$ d^{-1} [c]	
$k_D = 0.0105$ d^{-1} [c]	
$k_E = 0.00263$ d^{-1} [c]	
$k_G = 0.00832$ d^{-1} [c]	

[a] Adapted from Lin and Liao [18].
[b] Estimated from Thomann et al. [19].
[c] Calculated based on Table 1.

bioaccumulation in rainbow trout is used to estimate a range of physiological model parameters. Results obtained from the model simulation via the preliminary database are compared to the laboratory uptake and depuration data obtained from Lin and Liao [18] for soft tissue and shell of *H. diversicolor supertexta* as well as for the alga *G. tenuistipitata* var. *liui* in water with food exposure experiments to calibrate the physiological parameters in order to estimate a consistent set of parameters.

An initial set of parameters was estimated and then modified to reproduce the observed uptake and depuration characteristics for soft tissue, shell and algae. The remaining parameters for the other organs were also carefully calibrated simultaneously to meet the favorable agreement against the observed uptake and depuration data. It is recognized that the final set of parameters used to calibrate the data are hardly unique, but the parameter set is believed to represent a reasonable estimation for the model as a whole.

The numerical integration scheme used to solve the linear dynamic Eq. (1) is a subroutine based on the fourth-order Runge–Kutta and Euler predictor–corrector [20] and done in GWBASIC on a personal computer. Integration over time is straightforward in principle but is complicated by the existence of a large number of widely differing time scales. The algorithm is stable provided the error and convergence criterion are carefully monitored.

Fig. 5 displays the results of the model comparisons to the measured data of the temporal change in the laboratory Zn concentrations in soft tissue and shell of *H. diversicolor supertexta* as well as in algae during uptake and depuration periods for water with food exposure experiments. Table 3 lists the final set of physiological model parameters used for *H. diversicolor supertexta* in the model implementation.

Blood exchange flow rates to the various organs were not available in the literature for the *H. diversicolor supertexta*. The estimates of the exchange flow rates shown in Table 3 therefore are based on the data of Thomann et al. [19] where the exchange rates to various organs were

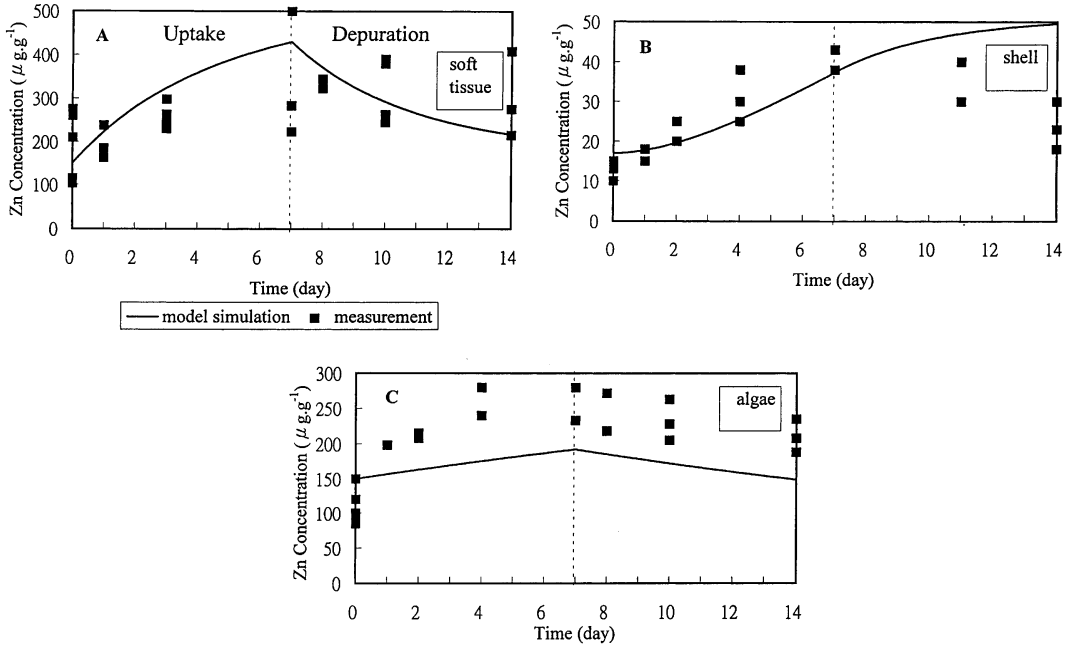

Fig. 5. Model simulation (lines) vs. experimental results (symbols) for (A) soft tissue, (B) shell, and (C) algae; during uptake and depuration periods in water with food exposure experiments.

Table 3
Physiological model parameters used for model implementation[a]

Binding Zn to plasma proteins $f_d = 0.2$ g l^{-1}
Gill partition coefficient $f_2 = 61300$ l kg^{-1} [b]
Soft tissue partition coefficient $f_3 = 5300$ l kg^{-1}
Gut wall partition coefficient $f_4 = 1300$ l kg^{-1}
Alimentary canal partition coefficient $f_5 = 6500$ l kg^{-1}
Shell partition coefficient $f_6 = 1000$ l kg^{-1}
Gill – water exchange $Q_{2w} = 0.01$ l d^{-1}
Gill – blood exchange $Q_{21} = 0.01$ l d^{-1}
Soft tissue – blood exchange $Q_{31} = 0.01$ l d^{-1}
Shell – blood exchange $Q_{61} = 0.01$ l d^{-1}
Gut wall – blood exchange $Q_{41} = 0.05$ l d^{-1}
Alimentary canal – gut wall exchange $Q_{45} = 0.07$ l d^{-1}
Gill sorption factor $\alpha_{w2} = 8$
Bile factor $\beta_{45} = 1$

[a] Values are adopted and estimated from Thomann et al. [19].
[b] kg = kg[wet].

carefully calibrated and were taken as being proportional to exchange flow on an l d^{-1} basis in the same proportion as that seen in rainbow trout.

4.2. Controller performance

The optimal PI controller for a trace Zn biomonitor control system can be expressed appropriately by Eq. (11) as,

$$\left\{\hat{U}(t)\right\} = \begin{bmatrix} [L_{11}] & [L_{12}] \\ [L_{21}] & [L_{22}] \end{bmatrix} \left\{ \int_0^t \left\{\hat{Z}(t)\right\} \mathrm{d}\tau | \left\{\hat{Z}(t)\right\} \right\}^{\mathrm{T}}$$
$$= [K_{\mathrm{PI}}] \left\{ \int_0^t \left\{\hat{Z}(t)\right\} \mathrm{d}\tau | \left\{\hat{Z}(t)\right\} \right\}^{\mathrm{T}}, \tag{12}$$

where $[K_{\mathrm{PI}}]$ may be referred to as a feedback PI controller gain matrix,

$$[K_{\mathrm{PI}}] = \begin{bmatrix} k_{11} & \cdots & k_{1,14} \\ \vdots & \ddots & \vdots \\ k_{71} & \cdots & k_{7,14} \end{bmatrix}. \tag{13}$$

Thus for the optimal PI controller, there are 98 feedback gain elements that need to be determined. The analyses of the controller performance were done in PC-MATLAB: *Control System Toolbox* [21]. The first step in the performance investigation is to determine matrices $[K]$, $[B]$, and $[H]$ of system control model in Eq. (14). The determination of $[K]$ and $[B]$ are followed by the definitions already presented in Eqs. (4) and (5). Matrix $[H]$ in the output relationship ($\{Z\} = [H]\{X\}$) is selected as a diagonal matrix: $[H] = \mathrm{diag}[h_{11}, h_{22}, \ldots h_{77}]$. The entries of $[H]$ for h_{33}, h_{66}, and h_{77} may be obtained from the results of model calibration between model predictions and measurements based on an uptake and depuration data for water with food exposure experiment (Fig. 5). The resulting values are: $h_{33} = 1.14$, $h_{66} = 1.22$ and $h_{77} = 1.34$. Because no available comparisons for other organ compartments could be found, it is assumed that $h_{ii} = 1$, for $i = 1$, 2, 4, and 5.

Having defined the matrices $[K]$, $[B]$, and $[H]$; the qualitative analysis of the system control model including stability, controllability, and observability can then be verified. Stability analysis indicates that eigenvalues of matrix $[K]$ are all negative: $\lambda_k = -30.64, -158.94, -252.31,$

$-157.55, -34.84, -0.0588$, and -6.36 for $k = 1, 2, \ldots, 7$. Hence, the system is stable. The results of controllability and observability analyses show that $|[\Xi][\Xi]^{\mathrm{T}}| \neq 0$ and $|[\Theta][\Theta]^{\mathrm{T}}| \neq 0$, i.e., controllability and observability of the system are assured.

Next the effects of weighting matrices $[S]$ and $[R]$ in the quadratic cost function are investigated. Usually $[S]$ and $[R]$ are selected to be diagonal in order to secure the robustness properties of the system [22]. The corresponding scalar expression of the quadratic cost function for a six-compartment PBPK model for *H. diversicolor supertexta* in an optimal PI feedback biomonitor control system can be obtained from Eq. (9) as,

$$J = \frac{1}{2}\int_0^\infty \left(s_{11}Z_1^2 + s_{22}Z_2^2 + \cdots + s_{77}Z_7^2 + r_{11}\dot{U}_1^2 + r_{22}\dot{U}_2^2 + \cdots + r_{77}\dot{U}_7^2\right) \mathrm{d}t. \tag{14}$$

Weighting matrices may be chosen in the following way to achieve specific performance bounds [23],

$$\int_0^\infty Z_i^2(t)\,\mathrm{d}t \leqslant \sigma_i^2, \quad \int_0^\infty U_i^2(t)\,\mathrm{d}t \leqslant \mu_i^2, \;\; i = 1, 2, \ldots, 7, \tag{15}$$

where σ_i and μ_i are the bound coefficients in that the root mean squared (RMS) values of the multiple outputs and inputs can be used to determine the performance bounds,

$$Z_{i\mathrm{RMS}} = \left(\int_0^\infty Z_i^2(t)\,\mathrm{d}t\right)^{1/2}, \quad U_{i\mathrm{RMS}} = \left(\int_0^\infty U_i^2(t)\,\mathrm{d}t\right)^{1/2}, \;\; i = 1, 2, \ldots, 7. \tag{16}$$

Because Z_i, U_i and $\dot{U}_i$ are of different orders of magnitude, some approximate scaling factor need to be used in selection of s_{ii} and r_{ii} [22]. These scaling factors are selected so that all terms representing derivations in state variables in the intergrands of objective equations are of the same order of magnitude. For simplicity, all terms representing deviations in control variables (or in their time derivatives) are the same order of magnitude. Because no general criterion could be found, it is assumed U_i^2 and $\dot{U}_i^2$ are of the same magnitude; thus $U_{i\mathrm{RMS}}^2 \cong \dot{U}_{i\mathrm{RMS}}^2$.

Particularly, it may be necessary to simultaneously limit the RMS values of output state variables as, $Z_{3\mathrm{RMS}}$(soft tissue) $\leqslant 100\ \mu\mathrm{g\ g}^{-1}$, $Z_{6\mathrm{RMS}}$(shell) $\leqslant 50\ \mu\mathrm{g\ g}^{-1}$, $Z_{7\mathrm{RMS}}$(algae) $\leqslant 50\ \mu\mathrm{g\ g}^{-1}$ of Zn concentration; and for the other compartments, $Z_{i\mathrm{RMS}} \leqslant 100\ \mu\mathrm{g\ g}^{-1}$ for $i = 1, 2, 4$, and 5. The RMS values of control input variables, i.e., for the Zn concentration in the ambient water, $U_{i\mathrm{RMS}} \leqslant 0.5\ \mathrm{mg\ l}^{-1}$.

Having determined the values of $Z_{i\mathrm{RMS}}$ and $U_{1\mathrm{RMS}}$, the elements in the weighting matrices can be calculated as follows by a scaling method. Therefore, in Eq. (14), let $s_{11}Z_{1\mathrm{RMS}}^2 = s_{22}Z_{2\mathrm{RMS}}^2 = \cdots = s_{77}Z_{7\mathrm{RMS}}^2$, then $s_{ii}/s_{jj} = Z_{j\mathrm{RMS}}^2/Z_{i\mathrm{RMS}}^2$. As a result, $s_{11} = s_{22} = \cdots = s_{55}$, $s_{66} = s_{77} = 2s_{55}$. In this work, r_{11} is kept constant throughout at 1, and only s_{11} is varied. Thus in this performance investigation, it is only necessary to adjust s_{11} which served as a tuning parameter, while the other weighting elements are fixed by the above noted scaling factors.

Fig. 6 shows the responses of the temporal change of Zn concentrations in algae, gill, and in the key organs of alimentary canal and gut tissue, respectively for the model simulation under no control action. Fig. 6A shows the gut tissue and alimentary canal are calculated to reach a steady-state at about 6 days, while at within about 11 days for gill and algae. Fig. 6B indicates that a steady-state Zn concentration for the soft tissue and the shell is not achieved. Fig. 6 also shows that the maximum Zn concentration in the gut tissue is about 2 times the Zn concentration in the alimentary canal because of the small relative mass of the gut tissue.

Fig. 7 gives the simulated responses of Zn concentrations in the whole body of *H. diversicolor supertexta* under no control and an optimal PI feedback control efforts at tuning parameter

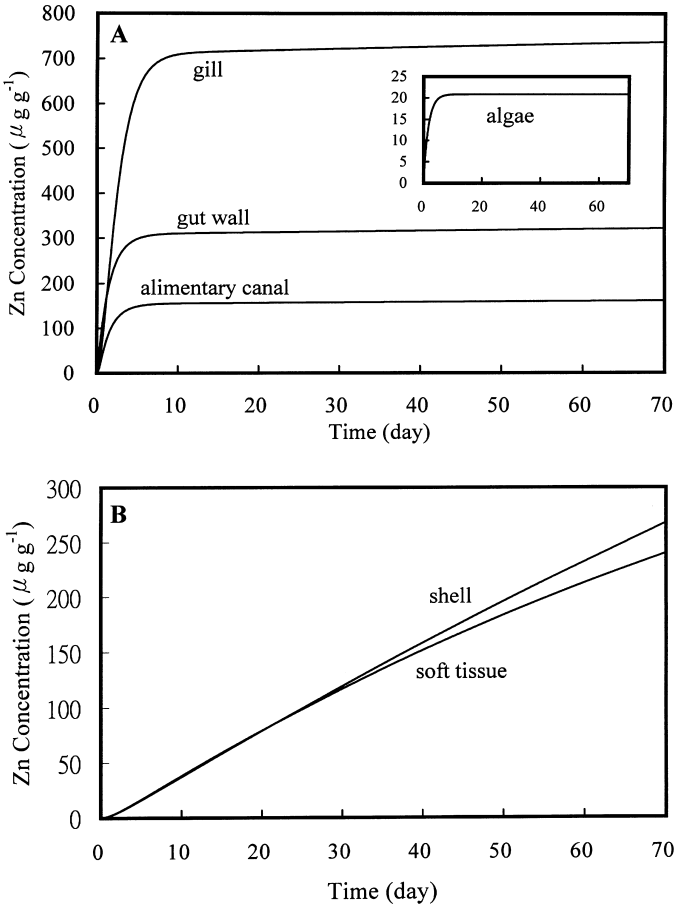

Fig. 6. Simulated temporal change of responses of Zn concentrations respectively in (A) algae, gill, gut tissue, and alimentary canal, and (B) shell and soft tissue; for model implementation under no control action.

$s_{11} = 0.1$, 0.5, and 1.0 with the desired equilibrium value shown as 10 μg g^{-1}. Fig. 8 shows the simulated responses of Zn concentrations in the key tissues of alimentary canal, plasma, and gut tissue of *H. diversicolor supertexta* under no control and an optimal PI feedback control action at $s_{11} = 1.0$ with the desired equilibrium state shown as 100 μg g^{-1}. These figures indicate that the responses were governed by the tuning parameter s_{11}. The success of these manipulations on control efforts can be achieved by adjusting the specified performance bounds for output and input variables to properly select the weighting matrices.

The evaluation of the optimal PI feedback control strategy presented above concludes that a satisfactory control of Zn concentrations in the metal biomonitor (*H. diversicolor supertexta*) system can be reached when the optimal feedback controllers are suitably tuned. Additionally, numerical results show that the optimal choice of tuning parameter s_{11} and the resulting costs vary with the desired equilibrium states.

5. Conclusions

A linear bioaccumulation dynamic model describing the behavior of Zn in the target tissues of a biomonitor (*H. diversicolor supertexta*) is developed based on a six-compartment PBPK model

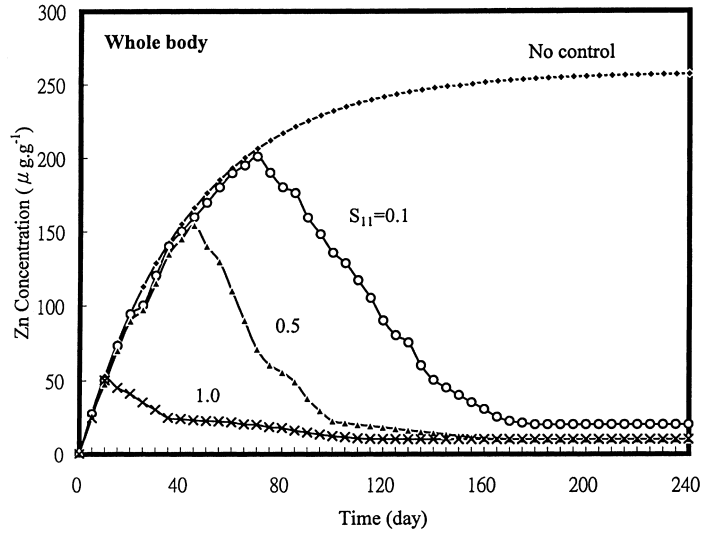

Fig. 7. Simulated temporal change responses of Zn concentrations in the whole body of *Haliotis diversicolor supertexta* under no control and an optimal PI feedback control action at $s_{11} = 0.1$, 0.5, and 1.0.

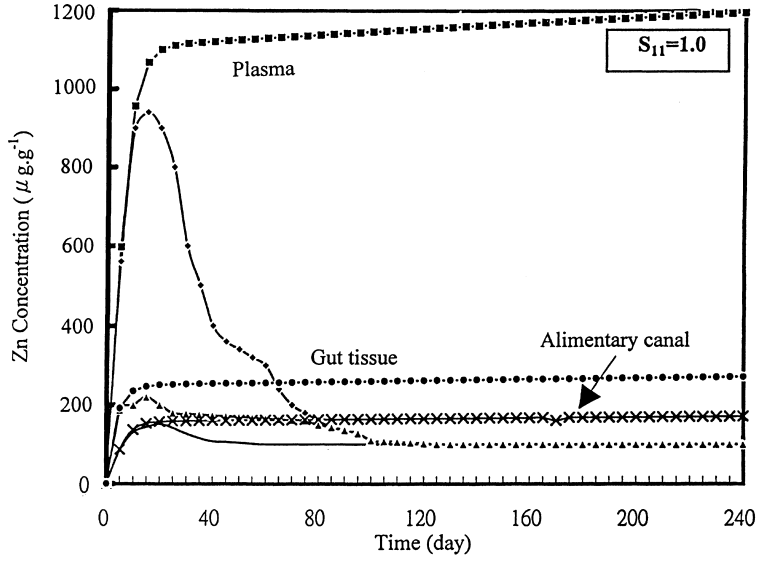

Fig. 8. Simulated temporal change responses of Zn concentrations in the key tissues of alimentary canal, plasma, and gut tissue of *Haliotis diversicolor supertexta* under no control and an optimal PI feedback control action at $s_{11} = 1.0$.

and is used in synthesizing the optimal feedback controllers for a trace metal biomonitor control system in an aquacultural ecosystem. For the model implementation, the input parameters for mollusc bioenergetics and physiological metal-specific processes are calibrated to observed pharmacokinetic data for the key compartments such as soft tissue and shell as well as for the algae in a 14 d uptake and depuration exposure experiment.

The optimization of the linear quadratic regulators (LQRs) with output feedback of a linear-invariant system is defined to determine an output feedback control loop such that the integral quadratic cost function meets its minimum value and the optimal PI controller is synthesized. The

optimal PI control strategy has been implemented to evaluate the dynamic behavior of Zn bioaccumulated in the target tissues of *H. diversicolor supertexta* and the specific results confirm that feedback control can be satisfactory in providing safe regulation of Zn concentrations over a wide range of target values.

More generally this paper has shown that the PBPK model incorporating the methodology of modern control engineering provides a scientific framework for discussion of designing a trace metal biomonitor control system in an aquacultural ecosystem.

Acknowledgements

The authors wish to acknowledge the financial support of the National Science Council of Republic of China under Grant NSC 87-2313-B-002-046.

Appendix A. Derivation of the optimal PI feedback control law in Eq. (11)

The derivative of Eq. (8) with respect to time yields:

$$\begin{aligned}
&\{\ddot{X}(t)\} = [K]\{\dot{X}(t)\} + [B]\{\dot{U}(t)\},\\
&\{X(0)\} = \{X_0\}, \quad \{U(0)\} = \{U_0\},\\
&\{\dot{X}(0)\} = [K]\{X_0\} + [B]\{U_0\},\\
&\{\dot{Z}(t)\} = [H]\{\dot{X}(t)\}
\end{aligned} \tag{A.1}$$

and defining the following new variables: $\{\omega\} \equiv \{\dot{X}\}, \{\theta\} \equiv \{\dot{U}\}, \{\xi\} \equiv \{\dot{Z}\}$. Thus, Eqs. (8) and (A.1) can be reduced to the following pair of vector-matrix differential equation:

$$\begin{aligned}
&\{\dot{X}(t)\} = \{\omega(t)\}, \quad \{X(0)\} = \{X_0\},\\
&\{\dot{\omega}(t)\} = [K]\{\omega(t)\} + [B]\{\theta(t)\},\\
&\{\omega(0)\} = [K]\{X_0\} + [B]\{U_0\},\\
&\{Z(t)\} = [H]\{X(t)\},\\
&\{\xi(t)\} = [H]\{\omega(t)\}.
\end{aligned} \tag{A.2}$$

Eq. (A.2) can be compactly expressed as:

$$\begin{aligned}
&\{\dot{\eta}(t)\} = [K_a]\{\eta(t)\} + [B_a]\{\theta(t)\}, \quad \{\eta(0)\} = \{\eta_i\},\\
&\{\zeta(t)\} = [H_a]\{\eta(t)\}.
\end{aligned} \tag{A.3}$$

where

$$\begin{aligned}
&\{\eta\} = \{\{X\}|\{\omega\}\}^{\mathrm{T}}, \quad \{\eta_i\} = \{\{X_0\}|\{\omega(0)\}\}^{\mathrm{T}}\\
&[H_a] = \mathrm{diag}[[H]|[H]], \quad \{\zeta\} = \{\{Z\}|\{\xi\}\}^{\mathrm{T}}\\
&[K_a] = \begin{bmatrix}[0] & [I]\\ [0] & [K]\end{bmatrix}, \quad [B_a] = \begin{bmatrix}[0]\\ [B]\end{bmatrix}.
\end{aligned}$$

Therefore, Eq. (9) in terms of the new variables becomes

$$J = \frac{1}{2}\int_0^{t_f} \left(\{\eta\}^{\mathrm{T}}[Q_a]\{\eta\} + \{\theta\}^{\mathrm{T}}[R]\{\theta\}\right) \mathrm{d}t, \tag{A.4}$$

where $[Q_a] = \mathrm{diag}[[Q][0]] = \mathrm{diag}[[H]^{\mathrm{T}}[S][H][0]]$. Matrix $[Q_a]$ becomes positive semidefinite since $[S]$ is positive semidefinite. Thus, the original output LQR in Eqs. (8) and (9) can be restated in Eqs. (3) and (A.4). The solution of the optimal control vector is given by the well-known expression

$$\{\hat{\theta}(t)\} = -[R]^{-1}[B_a]^{\mathrm{T}}[P]\{\hat{\eta}(t)\}, \tag{A.5}$$

where $[P] = [P]^{\mathrm{T}}$ is the positive definite solution of the Riccati equation

$$[\dot{P}] = -[P][K_a] - [K_a]^{\mathrm{T}}[P] + [P][B_a][R]^{-1}[B_a]^{\mathrm{T}}[P] - [Q_a], \quad [P(t_f)] = 0. \tag{A.6}$$

If system (A.3) is observable and controllable, then as t_f approaches infinity in Eq. (A.3), a suboptimal controller design followed by LQR algorithm in Eq. (7) yields,

$$\{\hat{\theta}(t)\} = -[R]^{-1}[B_a]^{\mathrm{T}}[P^*]\{\hat{\eta}(t)\} = -[R]^{-1}[B_a]^{\mathrm{T}}[P^*][H_a]^{-1}\{\zeta(t)\}, \tag{A.7}$$

where $[P^*] = [P^*]^{\mathrm{T}}$ is the unique, positive definite soultion of the following algebraic Riccati equation: $-[P^*][K_a] - [K_a]^{\mathrm{T}}[P^*] + [P^*][B_a][R]^{-1}[B_a]^{\mathrm{T}}[P^*] - [Q_a] = 0$.

Integrating Eq. (A.7) with respect to time and using the relations of $\{Z\} = [H]\{X\}$ gives

$$\{\hat{U}(t)\} = [[L_{12}] + [L_{22}]][H]\{\hat{X}(t)\} + [[L_{11}] + [L_{21}]][H]\int_0^t \{\hat{X}(\tau)\}\,\mathrm{d}\tau, \tag{A.8}$$

where the elements $[L_{ij}]$ are appropriately partitioned submatrices of $\left[-[R]^{-1}[B_a]^{\mathrm{T}}[P^*][H_a]^{-1}\right]$. The optimal PI feedback control law in Eq. (11) therefore is derived.

References

[1] P.S. Rainbow, Heavy metals in marine invertebrates. in: R.W. Furness, P.S. Rainbow (Eds.), Heavy Metals in the Marine Environment, CRC Press, Boca Raton, FL, 1990, pp. 67–79.

[2] K. Simkiss, M. Taylor, A.Z. Mason, Metal detoxification and bioaccumulation in molluscs, Mar. Biol. Lett. 3 (1982) 187–201.

[3] D.R. Livingstone, Towards a specific index of impact by organic pollution for marine invertebrates – Mini-Review, Comp. Biochem. Physiol. [C] 100 (1991) 151–1555.

[4] A.R. Walsh, J. O'Halloran, Accumulation of chromium by a population of mussels (*Mytilus edulis* (L)). exposed to leather tannery effluent, Environ. Toxico. Chem. 17 (1998) 1429–1438.

[5] J.W. Short, J.L. Sharp, Tributyltin in bay mussels (*Mytilus edulis*) of the pacific coast of the united states, Environ. Sci. Tech. 23 (1989) 740–743.

[6] S. Winter, Cadmium uptake kinetics by freshwater mollusc soft body under hard and soft water conditions, Chemosphere 32 (1996) 1937–1948.

[7] P.T. Conory, J.W. Hunt, B.S. Anderson, Validation of a short-term toxicity test endpoint by comparison with longer-term effects on larval red abalone Haliotis rufescens, Environ. Toxico. Chem. 15 (1996) 1245–1250.

[8] A. Rodriguez-Ariza, N. Abril, J.I. Navas, G. Dorado, J. Lopez-Barea, C. Pueyo, Metal, mutagenicity, and biochemical studies on bivalve molluscs from spanish coasts, Environ. Molecular Mutagenesis 19 (1992) 112–124.

[9] M-N. Croteau, L. Hare, A. Tessier, Refining and testing a trace metal biomonitor (*Chaoborus*) in highly acidic lakes, Environ. Sci. Tech. 32 (1998) 1348–1353.

[10] M. Martin, P.J. Coughtrey, Biological Monitoring of Heavy Metal Pollution: Land and Air, Applied Science, London, 1993.

[11] H. Curtis, Biology, 5th ed., Worth, New York, 1989.

[12] D.R. Livingstone, Biological differences in field populations of the common mussel *Mytilus edulis* L. exposed to hydrocarbons: some considerations of biochemical monitoring, in: L. Bolis, J. Zadunaisky, R. Gilles (Eds.), Toxins, Drugs, and Pollutants in Marine Animals, Springer, Berlin, 1984, pp. 161–175.

[13] K. Walsh, R.H. Dunstan, R.N. Murdoch, Differential bioaccumulation of heavy metals and organopollutants in the soft tissue and shell of the marine gastropod *Austrocochlea constrita*, Arch. Environ. Contam. Toxicol. 28 (1995) 35–39.

[14] G. Schüürmann, B. Markert, Ecotoxicology: Ecological Fundamentals, Chemical Exposure, and Biological Effects, Wiley, New York, 1997.
[15] C.T. Chen, Linear System Theory and Design, Holt, Rhinehart & Winston, New York, 1984.
[16] L.A. Zadeh, C.A. Desoer, Linear System Theory, McGraw-Hill, New York, 1963.
[17] R.A. DeCarlo, Linear Systems, Prentice-Hall, Englewood Cliffs, NJ, 1989.
[18] M.C. Lin, C.M. Liao, ^{65}Zn(II) accumulation in soft tissue and shell of abalone Haliotis diversicolor supertexta via the alga Grarcilaria tenuistiptata var. liui and the ambient water, Aquaculture 178 (1999) 89–101.
[19] R.V. Thomann, F. Shkreli, S. Harrison, A pharmacokinetic model of cadmium in rainbow trout, Environ. Toxico. Chem. 16 (1997) 2268–2274.
[20] A. Constantinides, Applied Numerical Methods with Personal Computers, McGraw-Hill, New York, 1987.
[21] MATLAB, MATLAB Version 4 User's Guide. The Math Works, Natick, MA, 1995.
[22] B.O.D. Anderson, J.B. Moore, Optimal Control: Linear Quadratic Method, Prentice-Hall, Englewood Cliffs, NJ, 1990.
[23] R.E. Skelton, Dynamic Systems Control, Wiley, New York, 1988.
[24] F.A.P.C. Gobas, D.C.G. Muir, D. Mackay, Dynamics of dietary bioaccumulation and faecal elimination of hydrophobic organic chemicals in fish, Chemosphere 17 (1988) 943–962.
[25] R.V. Thomman, Bioaccumulation model of organic chemical distribution in aquatic food chains, Environ. Sci. Tech. 23 (1989) 699–707.
[26] R.V. Thomman, J.P. Connolly, Model of PCB in the Lake Michigan lake trout food chain, Environ. Sci. Tech. 18 (1984) 65–71.